Study of Li-ion diffusion in Li-Mg, Li-Zn, and Li-Sn alloys using transition path sampling in MLACS

Hoan Tran-Van[1]

Co-author

Prof. Gabriel Antonius[1]
Prof. François Allard[1,2]

[1]Département de Chimie, Biochimie et Physique, Institut de Recherche sur l'Hydrogène, Université du Québec à Trois-Rivières, Trois-Rivières, Québec, Canada
[2]INRS-UQTR Joint Research Unit in Materials and Technologies for Energy Transition

Ottawa, 2026/6

Outline

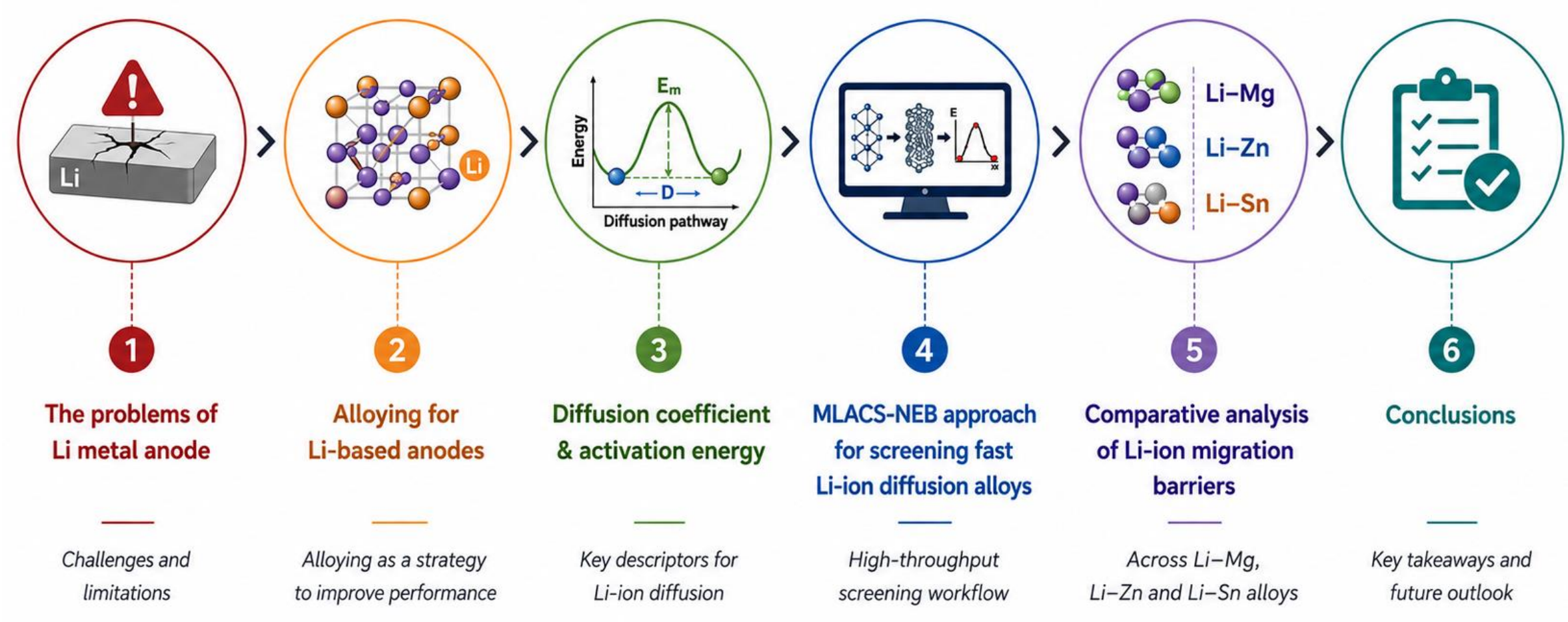
Li
Li
Energy
E_m
D
Diffusion pathway
E
xx
Li–Mg
Li–Zn
Li–Sn
1
2
3
4
5
6
The problems of Li metal anode
Alloying for Li-based anodes
Diffusion coefficient & activation energy
MLACS-NEB approach for screening fast Li-ion diffusion alloys
Comparative analysis of Li-ion migration barriers
Conclusions
Challenges and limitations
Alloying as a strategy to improve performance
Key descriptors for Li-ion diffusion
High-throughput screening workflow
Across Li–Mg, Li–Zn and Li–Sn alloys
Key takeaways and future outlook

1. The problems of Li metal anode

All-solid-state Li-ion batteries

High energy density, **safety**, recyclability

EV demand: > 300 km + fast charging [1]

Why Li metal anode?

High theoretical capacity**: 3860 mAh g^{-1}**

Lowest electrochemical potential: −3.04 V vs SHE

Lowest density: 0.534 g cm^{-3}

EV - Electric Vehicles
SHE - Standard Hydrogen Electrode
SEI – Solid electrolyte interphase

Challenges of Li metal anode

Dendrite growth → short circuit, safety risk

Dead Li and **void** formation → capacity loss

Unstable SEI → side reactions, low efficiency

Volume change → interface degradation

Critical limitations of Li metal anodes [2]

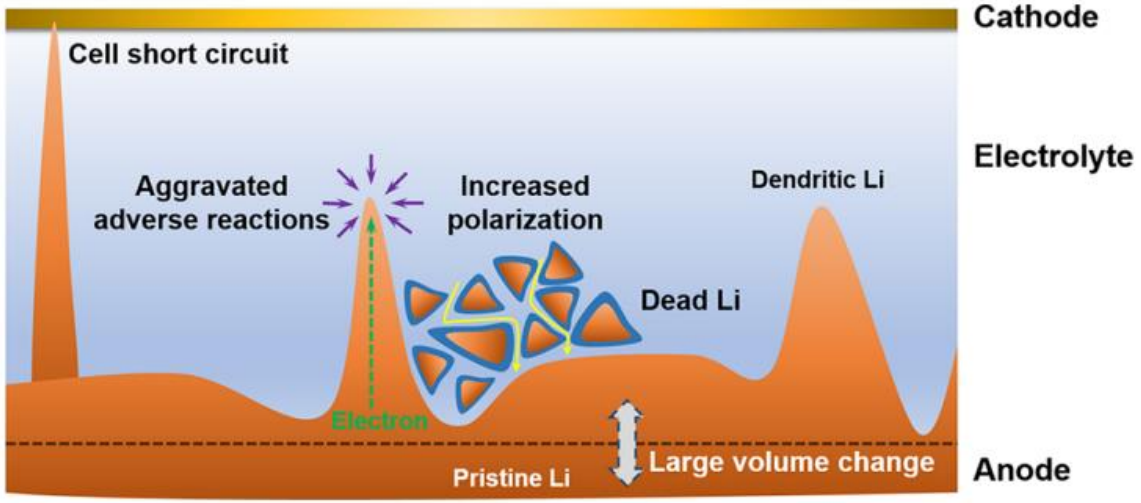

Li diffusion is a critical factor influencing the stabilization

[1] M.M. Islam et al., Phys. Chem. Chem. Phys., 17, 3383-3393 (2015)
[2] X.B. Cheng et al., Chem. Rev. 117 (2017) 10403–10473

2. Alloying for Li-based anodes

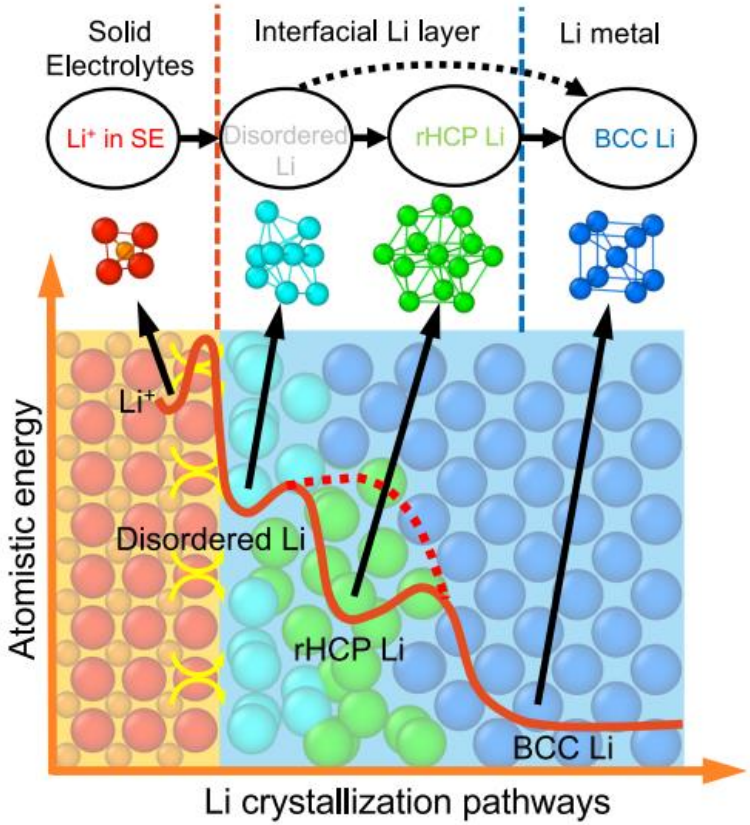

A diagram illustrating the multi-stage process of Li crystallization [3]

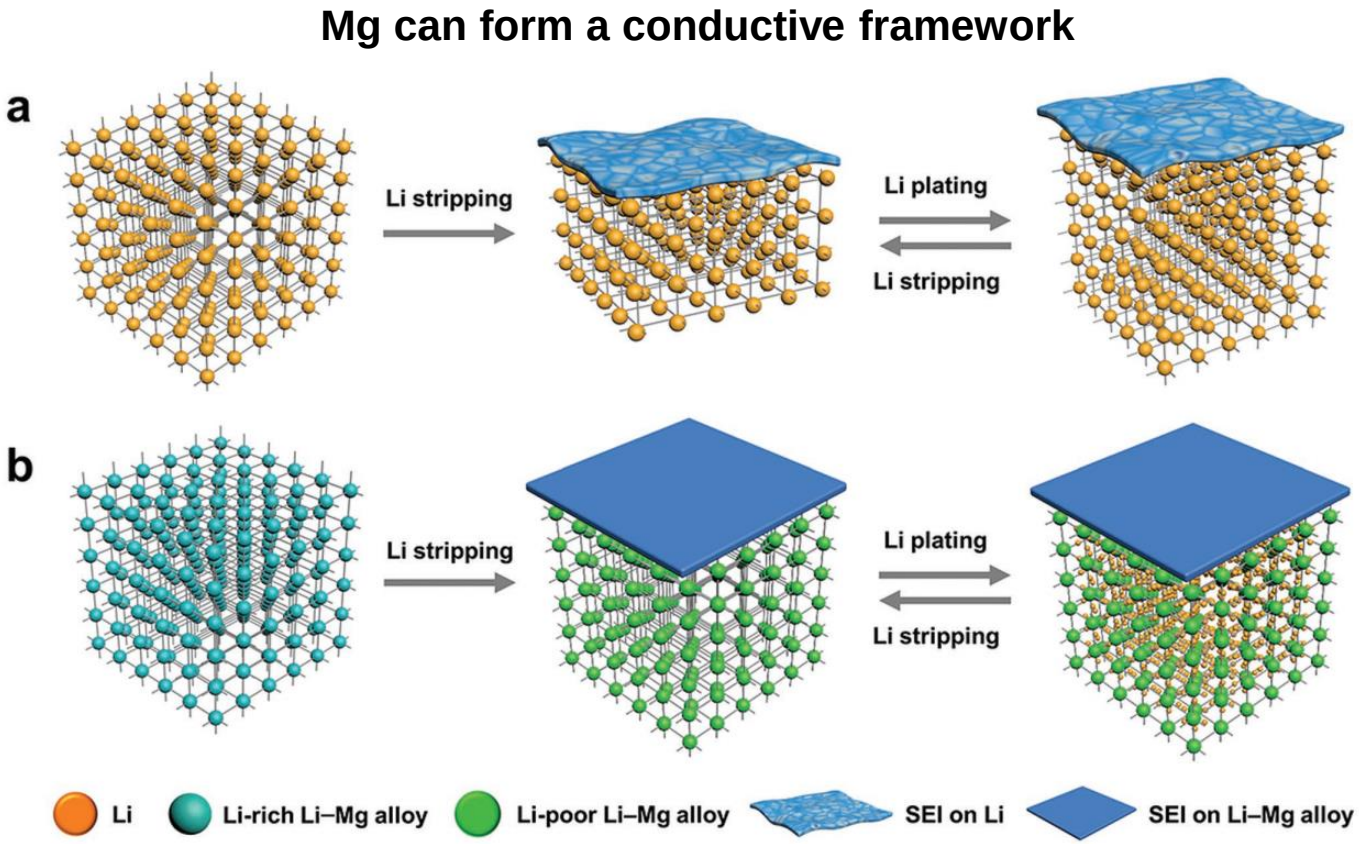

(a) Li and (b) Li–Mg anode structures, bulk & surface, during stripping/plating [4]

[3] M. Yang et al., Nat. Commun., 14, 2986 (2023)
[4] L. L. Kong et al., Adv Funct Mater., 29(13), 1808756 (2019)

Predict how alloying effectively changes diffusion and stability?

2. Alloying for Li-based anodes

Li-Mg

- Low Li diffusion
- **Structural integrity**

→ uniform Li deposition [4]

Li-Zn

- **Faster Li diffusion than Li**
- Low capacity [6]
- Buffer/protection layer for Li metal → uniform Li deposition [6, 8]

Li-Sn

- **Faster Li diffusion than Li**
- Volume change [9]
- Uniform transportation of the Li ions [9]

Li diffusion coefficients D_{Li}

Phase	Li Im-3m	Li-Mg (70-90 at%Li)
D_{Li} ($cm^2\ s^{-1}$)	1.6×10^{-10} [7]	$1.4\text{-}2.6\times10^{-10}$ [7]

Phase	LiZn Fd-3m	Li_7Sn_3 $P2_1/m$
D_{Li} ($cm^2\ s^{-1}$)	$8.8\text{-}37\times10^{-10}$ [5]	$3\text{-}5\times10^{-7}$ [5]

Alloy anode

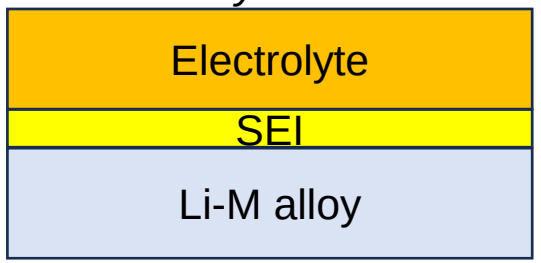

Alloy as a buffer layer

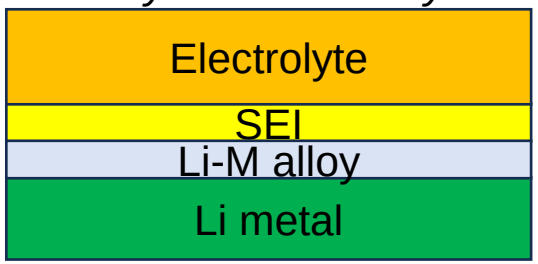

[5] Y. Huang et al., J. Mater. Chem. A, 10, 12350 (2022)
[6] X. Gu et al., Engineering Reports, 2021;3:e12339.
[7] M. Siniscalchi et al., ACS Energy Lett., 7, 3593 (2022)
[8] Q. Chen et al., ACS Appl. Mater. Interfaces, 13, 9985−9993 (2021)
[9] A. Serikkazyyeva et al., J. Alloys Compd., 965, 171381 (2023)

Enhanced Li diffusion can contribute to suppressing void and dendrite formation.

3. Diffusion coefficient & activation energy

The diffusion coefficient: $D = D_0 \exp\left(-\frac{E_f^{vac} + E_m}{k_B T}\right)$

The activation energy: $E_a = E_f^{vac} + E_m$

D_0: the pre-exponential factor
E_m: the migration energy for hopping
E_f^{vac} : the Li vacancy formation energy
E_a: the effective activation energy for Li diffusion

E_f^{vac} can be obtained from DFT calculations

E_m can be obtained from NEB method

Kinetically resolved activation (KRA) barrier [10]

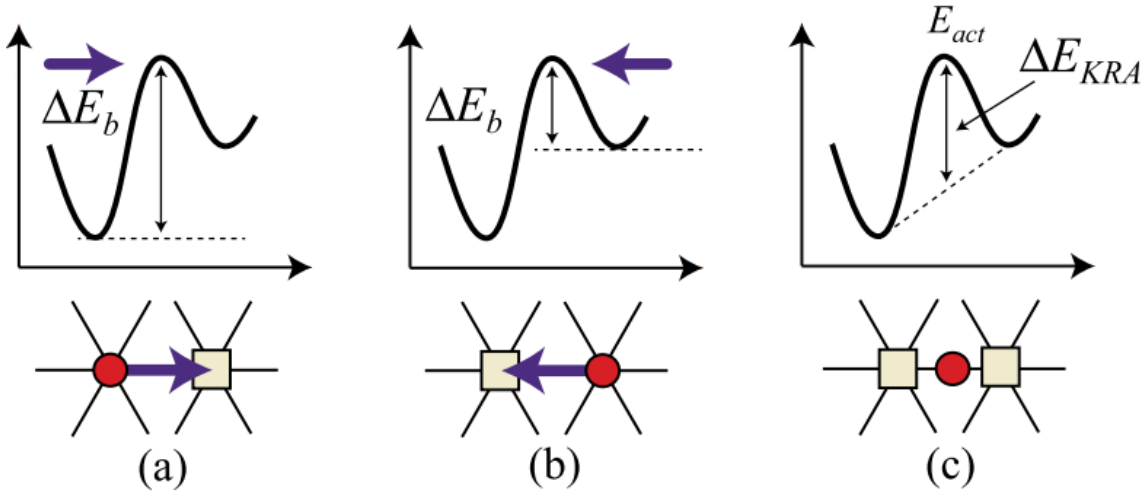

Forward hop | Reverse hop | ΔKRA = E_m

Focus on migration barrier E_m

- DFT - Density Functional Theory
- NEB – Nudged Elastic Band method

[10] A. Van der Ven et al., Chem. Rev., 120, 14, 6977–7019 (2020)

4. MLACS-NEB approach for screening fast Li-ion diffusion alloys

MLIPs address the trade-off issue

DFT-NEB

- Higher accuracy
- Higher computational costs for large supercell

MD-NEB

- Accuracy limited by interatomic potential
- Lower computational costs for large supercell

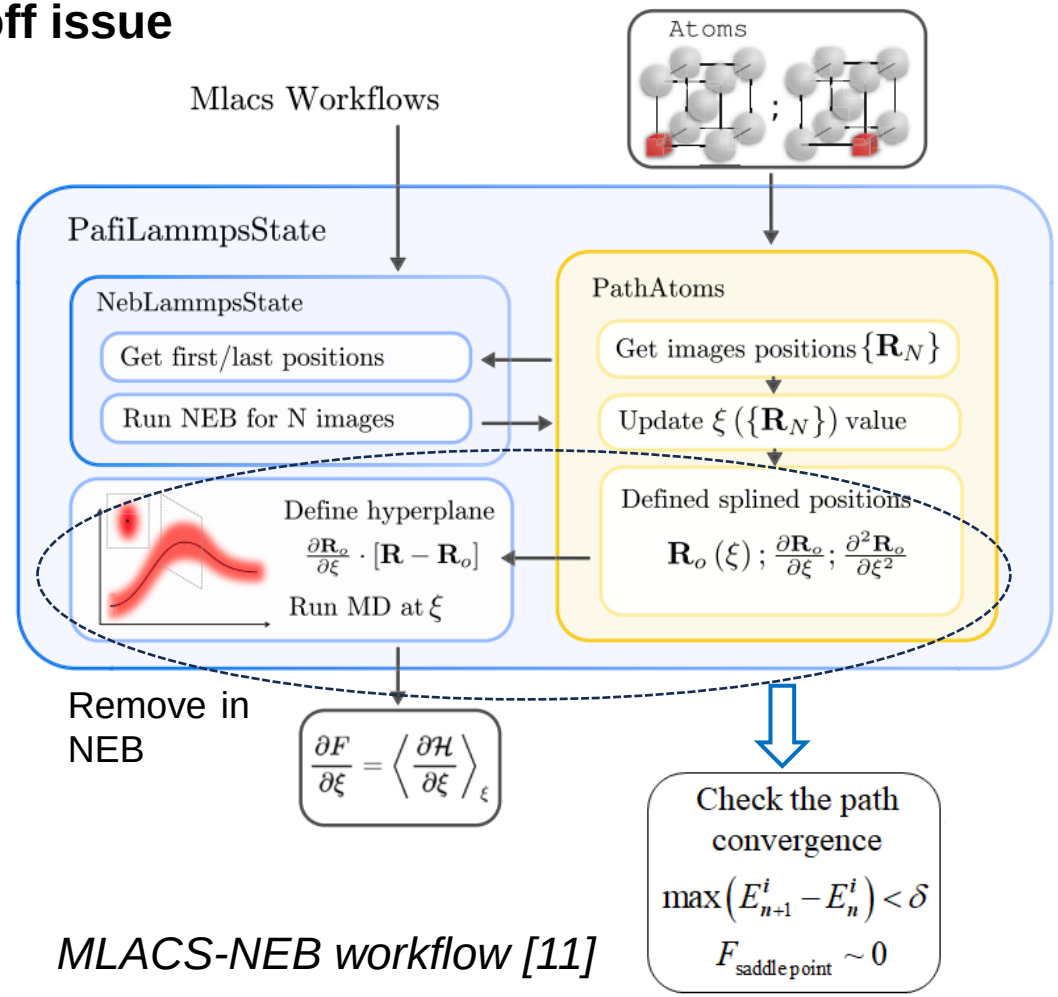

MLACS-NEB workflow [11]

- MD – Molecular Dynamics method
- MLIPs - Machine-learning interatomic potentials
- MLACS - Machine Learning Assisted Canonical Sampling

[11] A. Castellano et al., Comput. Phys. Commun., 316,109730 (2025)

4. MLACS-NEB approach for screening fast Li-ion diffusion alloys

- **10-30 training configurations**
- Linear SNAP
- **10–100× speed-up** compared to DFT-NEB

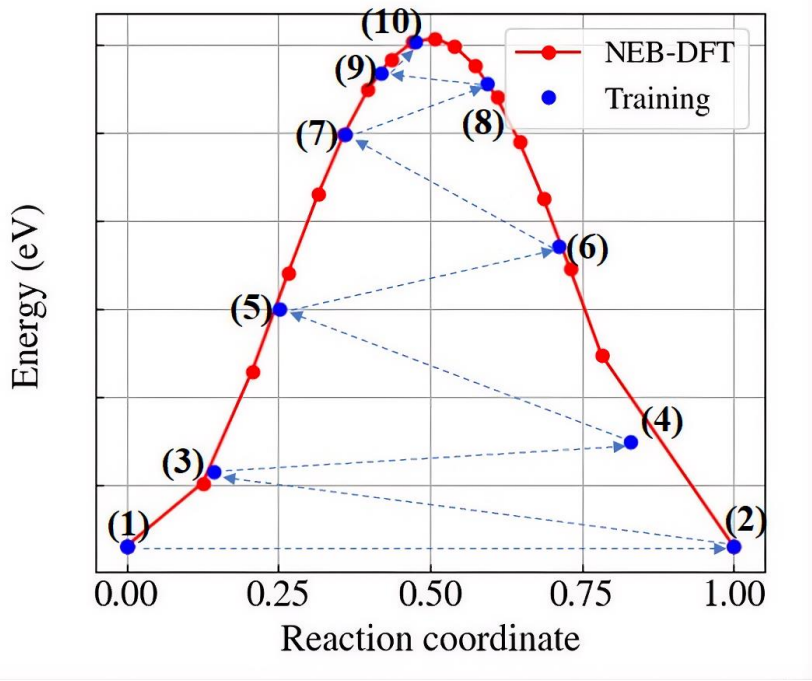

Sampling process and energy profile of training configurations for MLIP in the MLACS workflow.

Li, Im-3m, $|\Delta E_m|$= 8.17×10^{-4} eV

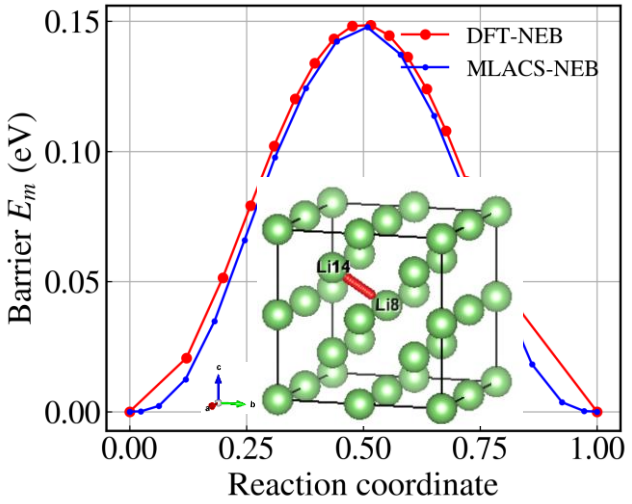

Li$_3$Mg, Fm-3m, $|\Delta E_m|$=1.29×10^{-3} eV

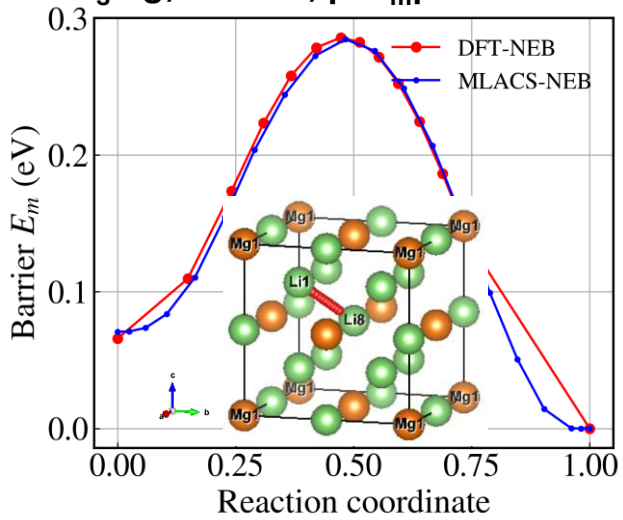

LiZn, Fd-3m, $|\Delta E_m|$= 1.34×10^{-4} eV

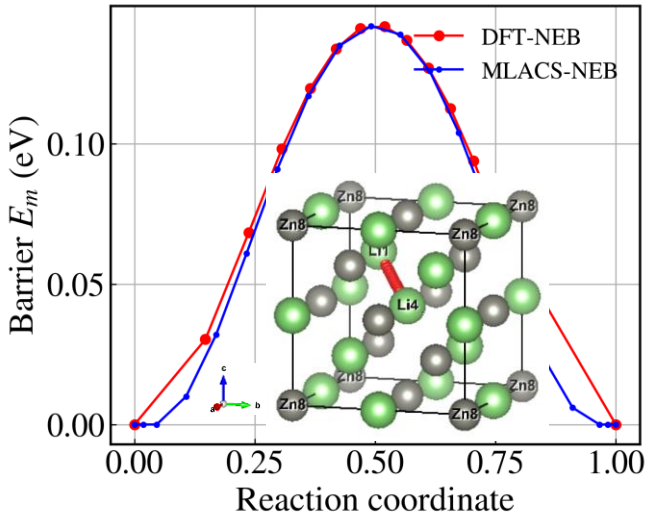

Li$_3$Sn, Fm-3m, $|\Delta E_m|$= 2.14×10^{-3} eV

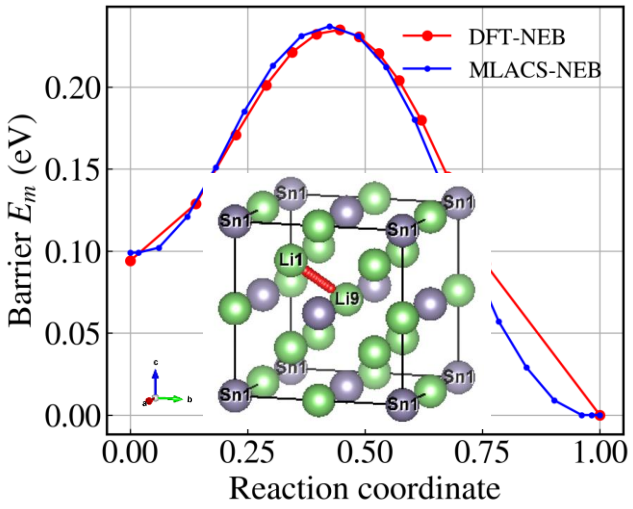

5. Comparative analysis of Li-ion migration barriers

❑ Convex hull and calculated structures

Convex hull of formation energies

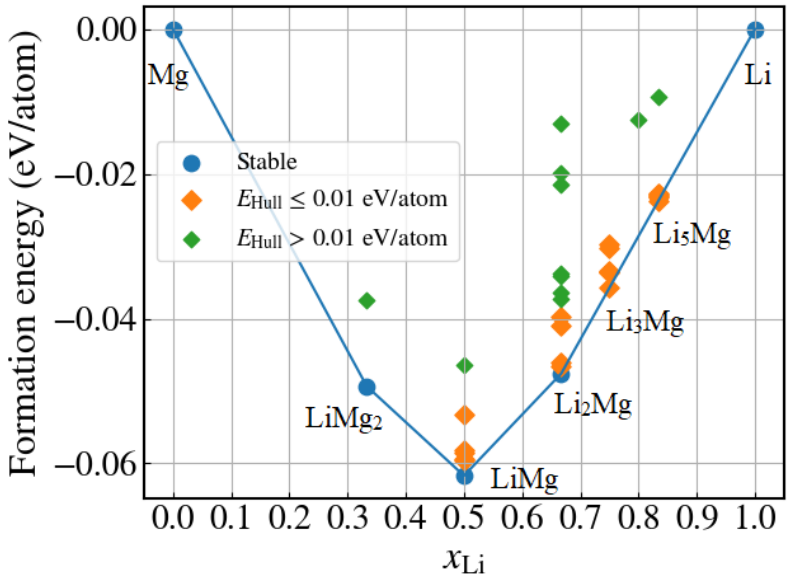

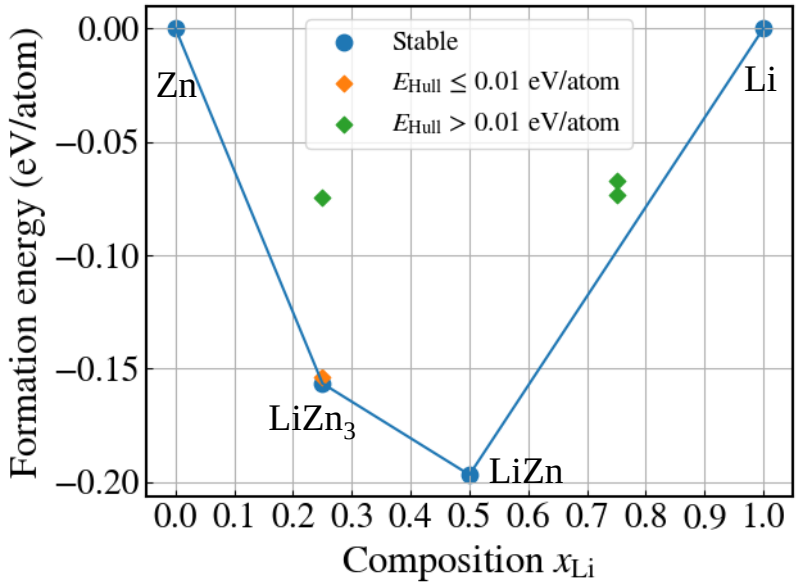

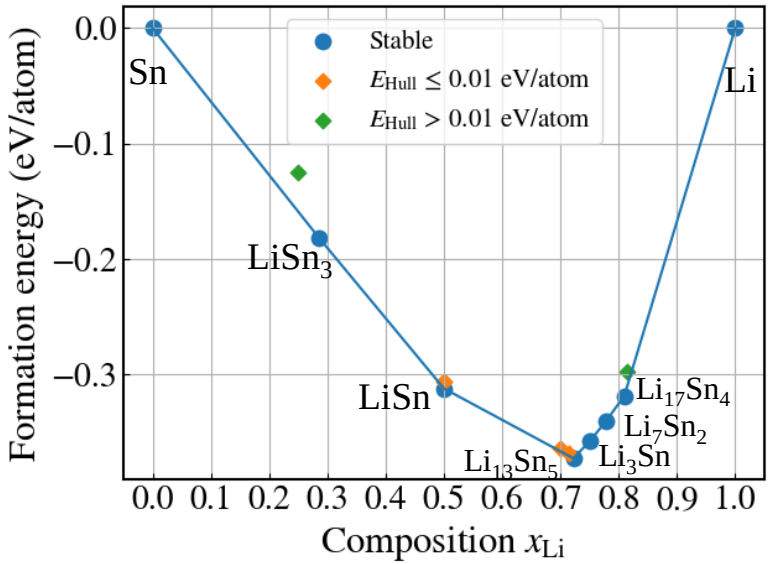

- LiMg (x_{Li} = 0.5): 6 polymorphs
- Li_2Mg (x_{Li} = 0.667): 5 polymorphs
- Li_3Mg (x_{Li} = 075) .: 6 polymorphs
- Li_5Mg (x_{Li} = 0.833): 5 polymorphs

Near-degenerate structures
→ **Boltzmann-weighted average**

- LiZn (x_{Li} = 0.5): 1 polymorphs

- Li_7Sn_2 (x_{Li} = 0.778): 1 polymorphs
- Li_3Sn (x_{Li} = 0.75): 1 polymorphs
- Li_5Sn_2 (x_{Li} = 0.714): 1 polymorphs
- LiSn (x_{Li} = 0.5): 2 polymorphs

5. Comparative analysis of Li-ion migration barriers

❑ The Li effective migration barrier

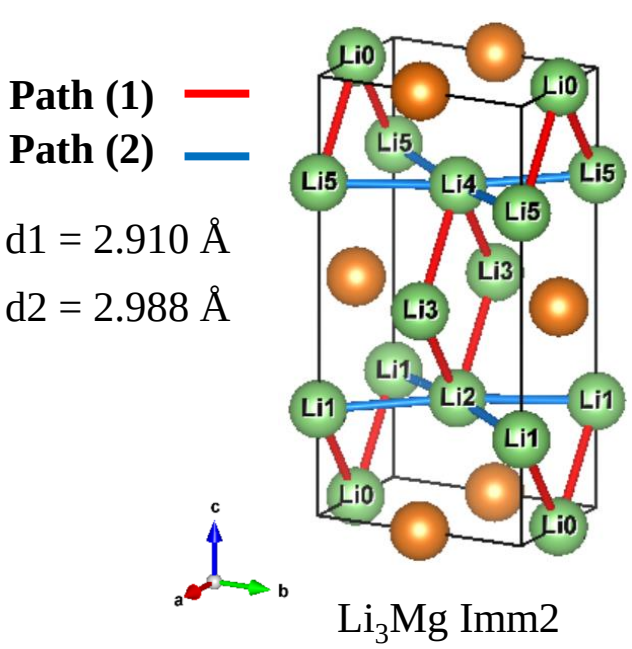

Li_3Mg Imm2

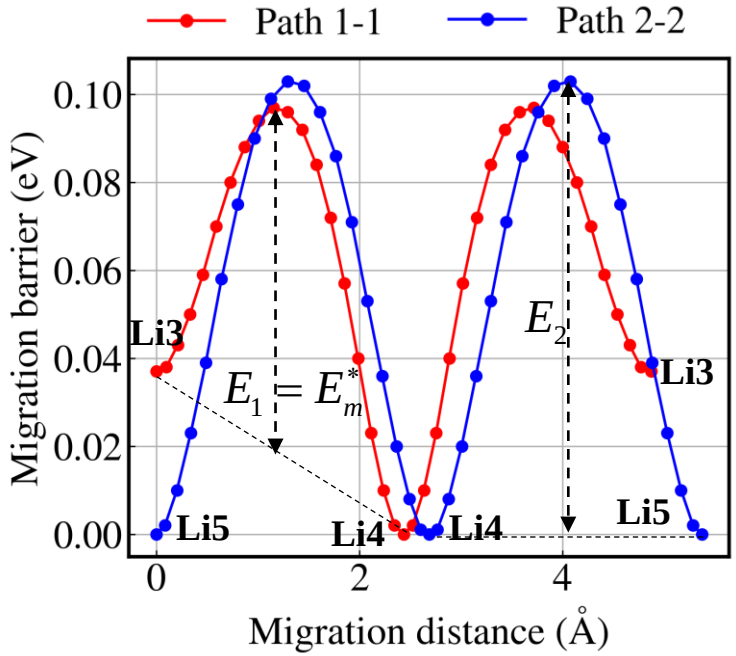

- Diffusion pathway selection
  - ➢ Li transport prefers lowest-energy migration path

Conventional cell structure of Li_3Mg (Imm2) with vacancy formation energies and MEP from MLACS-NEB.

5. Comparative analysis of Li-ion migration barriers

❑ The Li effective migration barrier

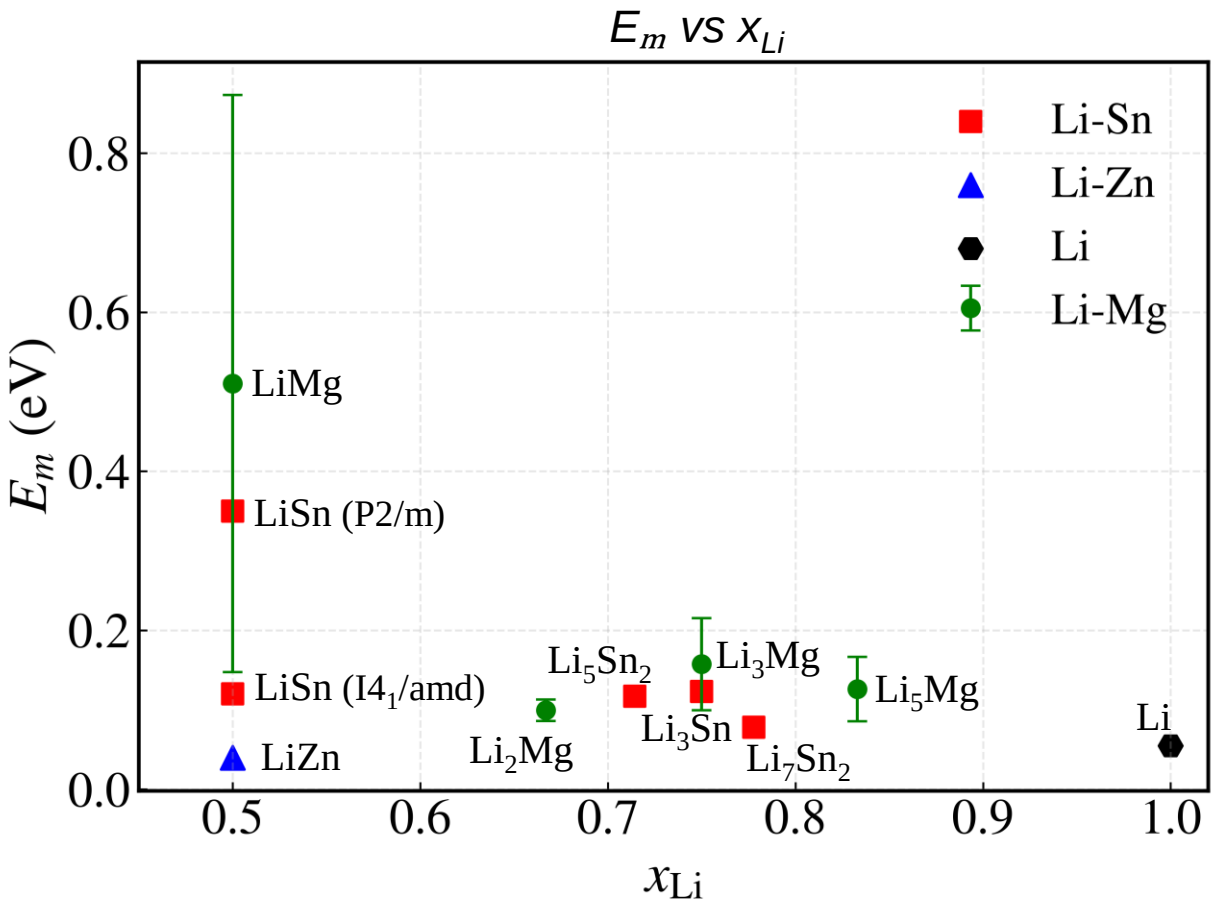

- Error bars indicate the **Boltzmann-weighted** standard deviation
- Supercells contain **108–256 atoms**, satisfying the shortest **vac-vac distance > 10 Å.**
- Linear SNAP with **$2J_{max}$ = 8 and r_{cut} = 5 Å**.

Minimum E_m in Li–Mg, Li–Sn, and Li–Zn systems

Phase	x_{Li}	E_m (eV)
Li_2Mg (mixed phase)	0.667	0.099
Li_7Sn_2 (Cmmm)	0.778	0.077
LiZn (Fd-3m)	0.5	0.040

- Very low E_m (0.04–0.1 eV) are accessible in Li–Mg, Li–Sn, and Li–Zn phases
- E_m is strongly structure-dependent
- No universal correlation between E_m and x_{Li} is observed.

5. Comparative analysis of Li-ion migration barriers

❑ Factors governing migration barriers

Coordination-Controlled Migration Barriers

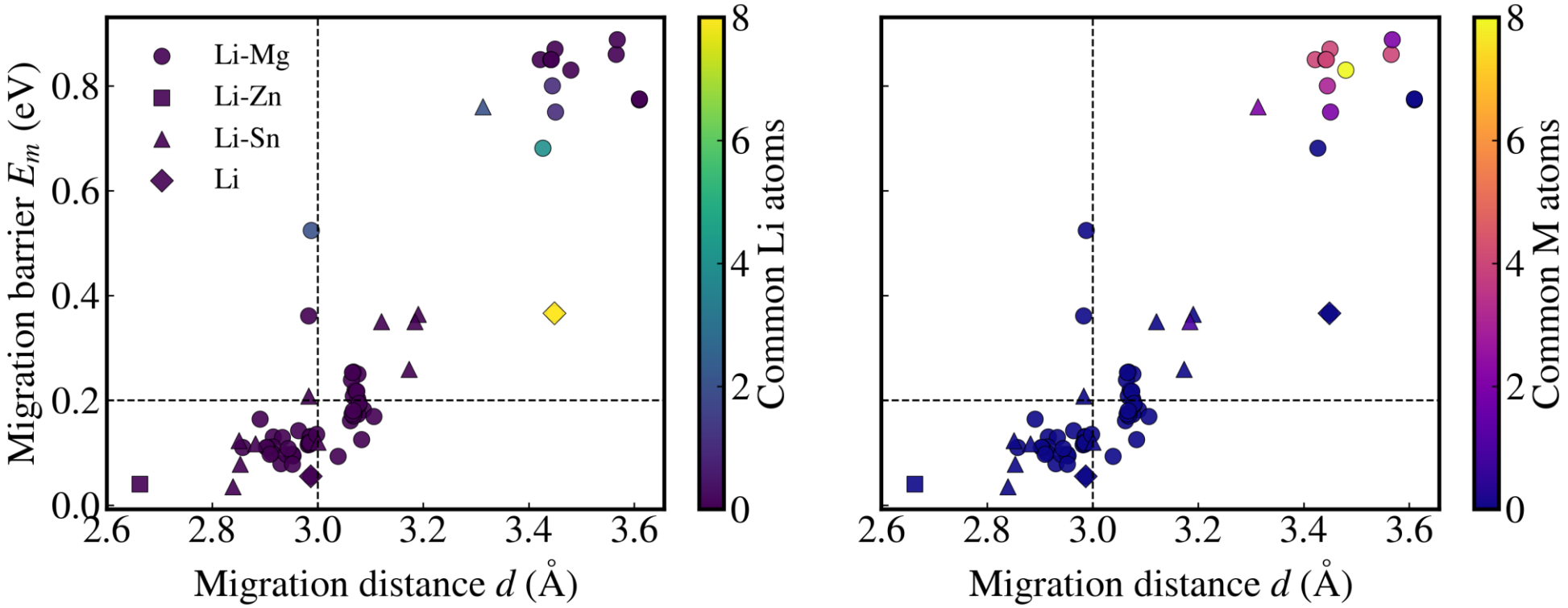

- Radius cutoff = 3.1 Å to determine coordination

- Low d → low E_m (baseline regime)
- Coordination overlap → barrier amplification

5. Comparative analysis of Li-ion migration barriers

❑ Factors governing migration barriers

Phase-dependent relationship between d and E_m

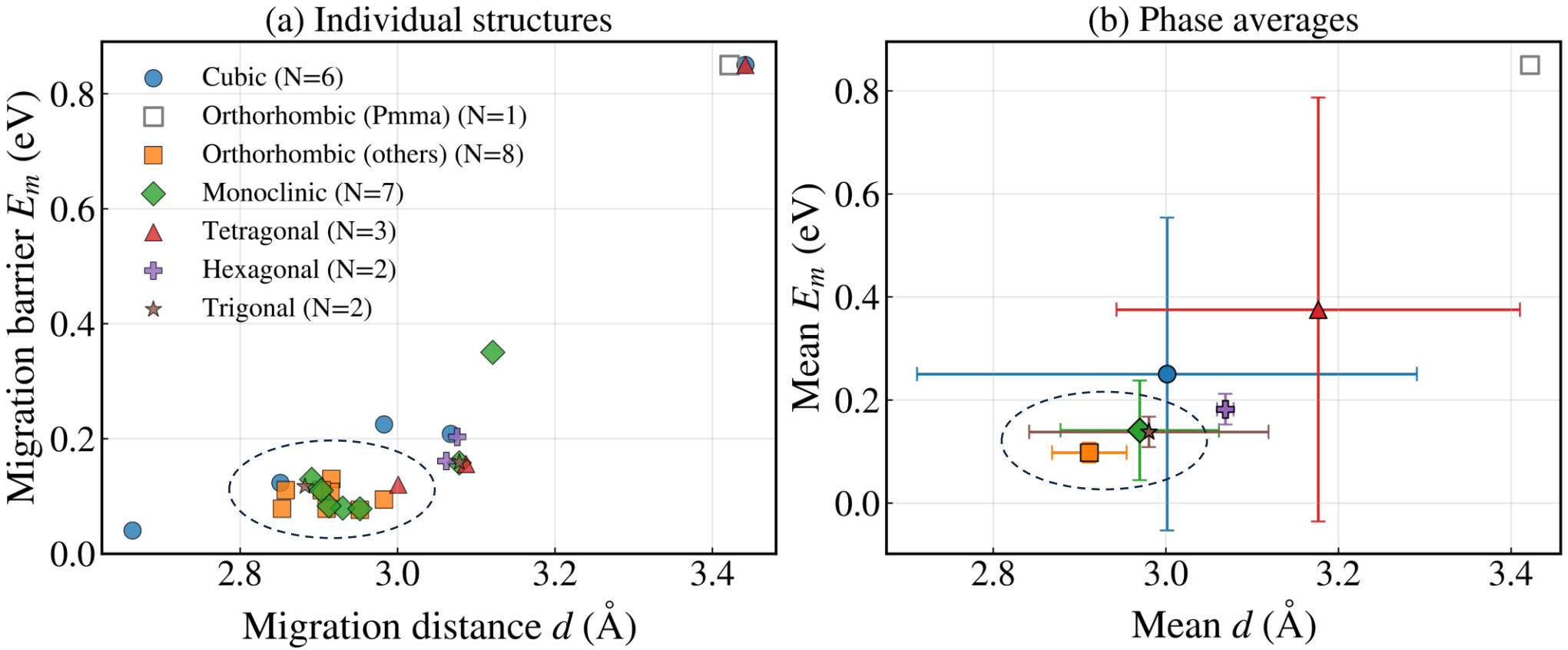

- Orthorhombic/monoclinic cluster at low *d* and low E_m.
- Phase indirectly reflects diffusion topology.

6. Conclusion

The obtained results

1. **MLACS-NEB** efficiently screens Li-ion migration barriers

2. **Li_2Mg, Li_7Sn_2 and LiZn** exhibit low Li migration barriers (E_m < 0.1 eV)

3. **Low E_m** is favored by **short migration distance** and the **absence of common neighboring atoms**

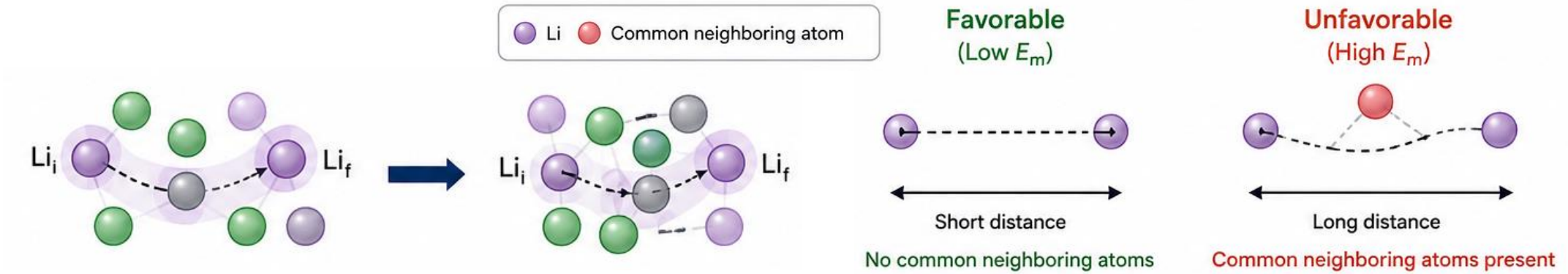

Future work

1. Complete NEB calculations with other crystal structures
2. Perform calculations with Li–Mg solid solution
3. Evaluate vacancy formation energy

Thank you

mlacs-developers